# Megalin-dependent cubilin-mediated endocytosis is a major pathway for the apical uptake of transferrin in polarized epithelia

Renata Kozyraki*, John Fyfe†, Pierre J. Verroust‡, Christian Jacobsen*, Alice Dautry-Varsat§, Jakub Gburek¶, Thomas E. Willnow∥, Erik Ilsø Christensen¶, and Søren K. Moestrup*,**

Departments of *Medical Biochemistry and ¶Cell Biology, Institute of Anatomy, University of Aarhus, DK-8000 Aarhus, Denmark; ‡Institut National de la Santé et de la Recherche Médicale U538, Centre Hospitalo Universitaire, St. Antoine, 75012 Paris, France; †Department of Microbiology, Michigan State University, East Lansing, MI 48824; §Institut Pasteur, 75015 Paris, France; and ∥Max-Delbrueck Center for Molecular Medicine, 13125 Berlin, Germany

Cubilin is a 460-kDa protein functioning as an endocytic receptor for intrinsic factor vitamin $B_{12}$ complex in the intestine and as a receptor for apolipoprotein A1 and albumin reabsorption in the kidney proximal tubules and the yolk sac. In the present study, we report the identification of cubilin as a novel transferrin (Tf) receptor involved in catabolism of Tf. Consistent with a cubilin-mediated endocytosis of Tf in the kidney, lysosomes of human, dog, and mouse renal proximal tubules strongly accumulate Tf, whereas no Tf is detectable in the endocytic apparatus of the renal tubule epithelium of dogs with deficient surface expression of cubilin. As a consequence, these dogs excrete increased amounts of Tf in the urine. Mice with deficient synthesis of megalin, the putative coreceptor colocalizing with cubilin, also excrete high amounts of Tf and fail to internalize Tf in their proximal tubules. However, in contrast to the dogs with the defective cubilin expression, the megalin-deficient mice accumulate Tf on the luminal cubilin-expressing surface of the proximal tubule epithelium. This observation indicates that megalin deficiency causes failure in internalization of the cubilin–ligand complex. The megalin-dependent, cubilin-mediated endocytosis of Tf and the potential of the receptors thereby to facilitate iron uptake were further confirmed by analyzing the uptake of $^{125}I$- and $^{59}Fe$-labeled Tf in cultured yolk sac cells.

I n nonintestinal tissues, transferrin (Tf) facilitates the cellular uptake of iron by the ubiquitous iron-regulated Tf receptor (TfR) and the homologous liver-specific Tf receptor-2 (TfR2) (1–3). Furthermore, phagocytes have a substantial iron uptake in relation to hemoglobin (4) and heme (5) metabolism. TfR-mediated endocytosis of Tf is generally considered to lead to unloading of Tf-bound iron in the cellular endosomes, whereas the receptors and the iron-free apoTf molecules recycle in intact form to the surface where they segregate (6). In addition to the TfR- and TfR2-mediated uptake of Tf, the existence of a third receptor pathway for Tf in some polarized epithelia seems likely. One important line of evidence for this comes from studies by Young *et al.* (7), who have shown that Tf is effectively endocytosed from the luminal (apical) surfaces of polarized yolk sac cells despite the basolateral membrane sorting of TfR in polarized epithelia (8, 9). Another line of evidence comes from the fact that the uptake of Tf in the yolk sac (7) and other organs such as the kidney (10) leads to catabolism of Tf.

The present study was initiated to identify ligands to cubilin, the 460-kDa receptor known to function as the intrinsic factor-vitamin $B_{12}$ (IF-$B_{12}$) receptor in the intestine (11, 12) and in kidney and yolk sac as the high-affinity apolipoprotein-A1/HDL receptor (13, 14) and low-affinity albumin receptor (15). Cubilin lacks a classical transmembrane region, and the membrane trafficking of cubilin is suggested to be assisted by megalin (16), which colocalizes with and binds to cubilin (11). Furthermore, the two receptors act in concert for ligand uptake (13–15, 17).

Using a cubilin-affinity approach, we discovered Tf as a novel ligand to cubilin. Subsequent investigations of the receptor-mediated uptake of Tf in the renal proximal tubules and in cultured yolk cells demonstrate that cubilin is a physiological and quantitatively important third Tf receptor involved in Tf catabolism and $Fe^{3+}$ uptake. Furthermore, this discovery made it possible to establish that the cubilin internalization depends on megalin.

## Materials and Methods

**Receptors, Antibodies, and Ligands.** Cubilin and megalin were purified from solubilized rabbit and human renal cortex as described (11). Tf was from Calbiochem. Polyclonal and monoclonal antibodies against rat cubilin and megalin have been described (18, 19). Polyclonal antibody against human Tf was from Dako and recognizes human, dog, and mouse Tf. Human apolipoprotein A1 was from Sigma. Porcine IF-$B_{12}$ was kindly donated by Ebba Nexø (Aarhus University Hospital). Receptor-associated protein (RAP) was produced as a recombinant protein in *Escherichia coli*.

Cubilin-affinity chromatography of human serum was carried out by using a cubilin-linked Sepharose-4B matrix as described (13). The eluted ≈80-kDa electroblotted band was cut out and subjected to amino-terminal sequencing by Edmann degradation on an Applied Biosystems 477 A sequencer. Tf-affinity chromatography of solubilized renal rat brush border was carried out by using a Tf-Sepharose-4B matrix. The affinity chromatography bed was prepared by coupling of human Tf (Sigma) to CNBr-activated Sepharose 4B (Amersham Pharmacia). Rat renal brush-border membranes were isolated as described (20). The Tf-Sepharose column (1.5 ml) was loaded with 30 ml of 1% Triton X-100 solubilized membranes (300 mg of protein) by overnight recirculation at 0.2 ml/min. After washing, the bound protein fraction was eluted with PBS, pH 5.0/10 mM EDTA/0.5% CHAPS (3-[(3-cholamidopropyl)dimethylammonio]-1-propanesulfonate). Collected 1-ml fractions were concentrated 10 times and analyzed by 4–16% SDS/PAGE.

**Immunohistochemical Analysis of Human, Canine, and Mouse Kidneys.** A strain of mixed-breed dogs exhibiting autosomal recessive inheritance of selective $B_{12}$ malabsorption has been characterized thoroughly (21). Megalin-deficient mice were produced by gene targeting disruption as described (22). Mouse kidneys were fixed by perfusion through the left ventricle of the heart, whereas
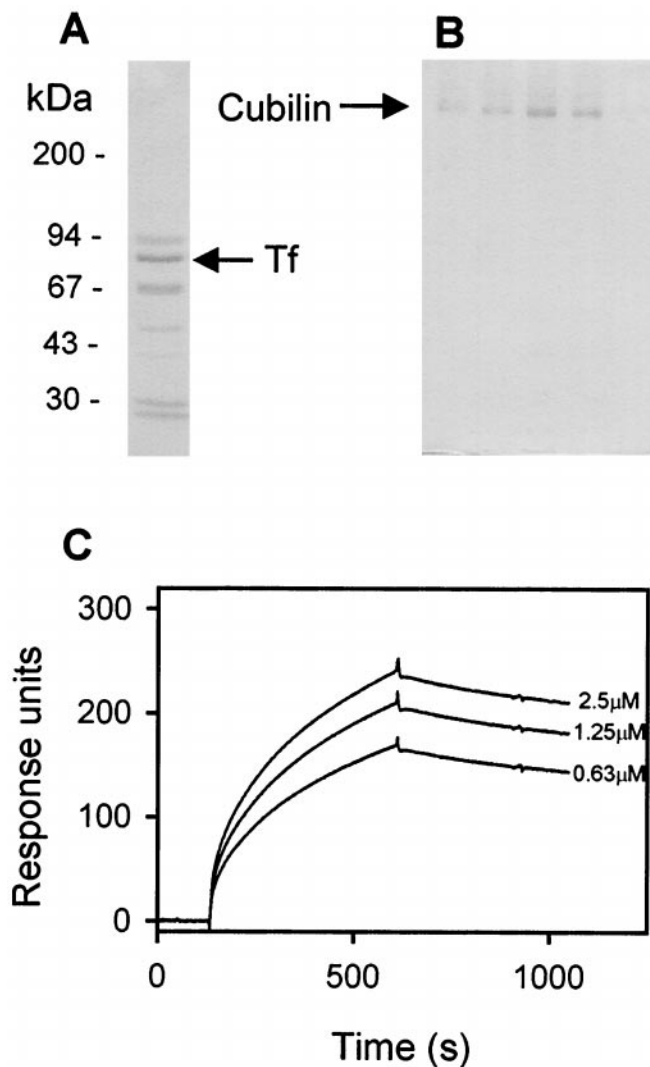
CELL BIOLOGY

**Fig. 1.** Identification of Tf as a cubilin ligand by affinity chromatography and surface plasmon resonance analysis. (*A*) SDS/PAGE and Coomassie staining of eluate from a cubilin-Sepharose column loaded with human serum. The band of Tf (identified by amino-terminal sequencing) is indicated. (*B*) SDS/PAGE and Coomassie staining of the eluate from a Tf-Sepharose column loaded with solubilized rat renal brush-border membranes. The band of cubilin (identified by immunoblotting) is indicated. (*C*) Surface plasmon resonance analysis of the binding of various concentrations of purified human Tf to immobilized cubilin.



**Fig. 2.** Distribution of cubilin and Tf in normal dog kidney, in dog kidney with deficient cubilin surface expression, and in normal human kidney as determined by immunohistochemistry. (*A*) Cubilin staining is largely seen in the apical region (arrow) of the proximal tubule of normal dogs. Two nuclei (N) are marked. (*B*) A granular-like intracellular staining pattern is seen in dogs with deficient surface expression of cubilin. (*C*) A punctate staining (arrow) for Tf is seen in the proximal tubule of control dogs. (*D*) No Tf labeling is detectable in the dogs with affected cubilin expression. (*E*) Intensive accumulation of punctate Tf staining (arrow) in the human proximal tubule. (*F*) Immunoelectron microscopy identifies the human Tf-labeled structures as typical lysosomes. Immunoperoxidase staining, ×1,000 (*A* and *E*) and ×900 (*B–D*); immunogold staining, ×35,000 (*F*).

dog kidneys were fixed by retrograde perfusion through the abdominal aorta. Normal, uninvolved human renal tissue was obtained from renal carcinoma kidneys. The fixatives used were 1–8% paraformaldehyde in 0.1 M sodium cacodylate buffer, pH 7.4.

For light microscope immunocytochemistry, 0.8-$\mu$m cryosections were incubated for 1 h with the primary antibody diluted 1:500 to 1:200,000 followed by incubation for 1 h with horseradish peroxidase-conjugated secondary antibody. The antibodies used were rabbit anti-rat cubilin IgG (19), sheep anti-rat megalin IgG (11), and rabbit anti-human Tf (Dako). Electron microscope immunocytochemistry was performed on 90-nm cryosections of incubated primary antibody diluted 1:20,000 to 1:200,000 followed by incubation with gold (10 nm) conjugated anti-rabbit secondary antibody. The sections were examined in a Philips CM100 electron microscope. Controls involving incu-
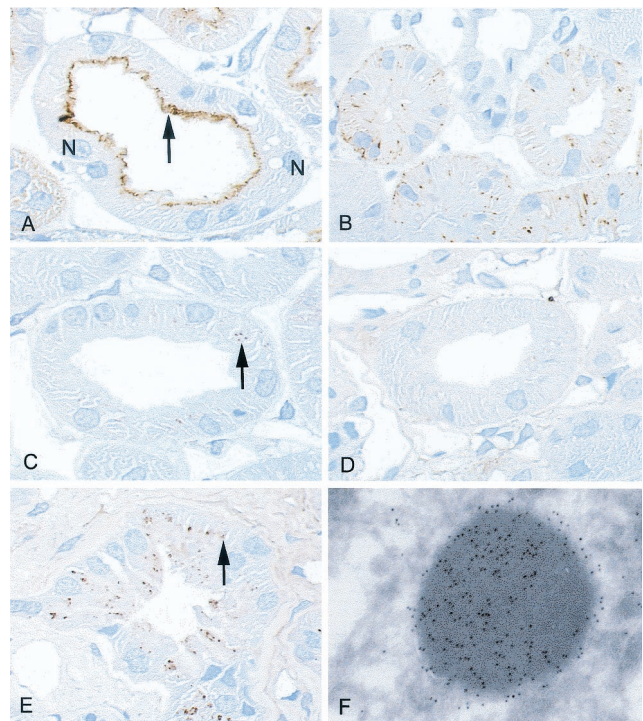
bation without primary antibody and incubation with nonspecific rabbit or sheep IgG revealed no significant labeling.

**Analysis of Human, Dog, and Mouse Urine and Plasma Samples.** The urine samples were collected and frozen as described (13, 23). No significant differences were measured in the urinary creatinine concentration in normal dogs versus cubilin-deficient dogs and in normal mice versus megalin-deficient mice. The urinary and plasma content of Tf was analyzed by immunoblotting by using polyclonal anti-human Tf antibody (Dako).

**Surface Plasmon Resonance Analysis.** Cubilin–Tf interactions were assessed by surface plasmon resonance analysis on a BIAcore 2000 instrument (Biacore, Uppsala, Sweden) as described (11), and binding kinetics were analyzed by using BIAEVALUATION software version 3.1 (Biacore). Human cubilin was immobilized to the chip surface at a density of 40 fmol/mm$^2$.

**Confocal Immunofluorescence Microscopy.** Brown Norway rat yolk sac epithelial cells transformed with mouse sarcoma virus (24) expressing cubilin and megalin were grown on four-chamber glass slides (Nunc), washed twice, and preincubated in serum-free MEM (GIBCO) containing 0.5% ovalbumin for 30 min at 37°C. After incubation at 4°C for 60 min in the above medium containing 40 $\mu$g/ml Alexa 594-conjugated human Tf (Molecular Probes), the cells were washed and further incubated at 37°C for 1, 5, 10, 15, or 30 min. At the end of the incubation period,
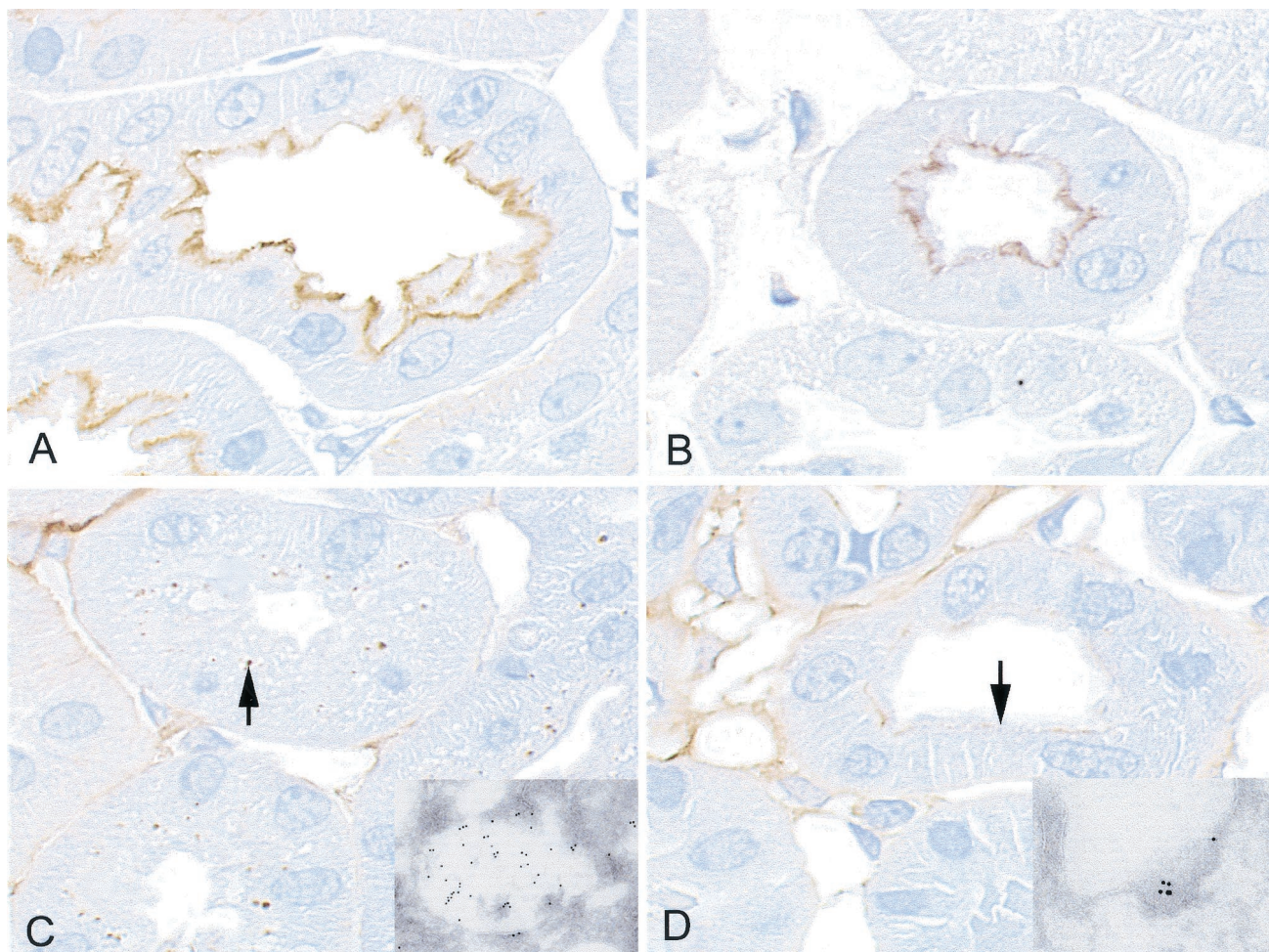
**Fig. 3.** Distribution of cubilin and Tf in kidneys from wild-type and megalin-deficient mice as determined by immunohistochemistry. (*A*) Staining for cubilin in the apical part of the proximal tubule in the wild-type kidney. (*B*) Expression of cubilin in the megalin-deficient kidney. (*C*) Tf staining is seen as a vacuolar staining (arrow) in the proximal tubule of the wild-type kidney. (*D*) The megalin-deficient kidney exhibits an apical plasma membrane staining (arrow) for Tf corresponding to the surface staining for cubilin (*B*). (*Insets*) Immunogold staining for Tf in the wild-type (*C*) and the megalin-deficient (*D*) kidney.

the cells were washed four times in PBS and fixed in 4% formaldehyde for 30 min at room temperature. After washing, the cells were incubated for 1 h in PBS (for nonpermeabilized cells) or PBS/Triton 0.05% (for permeabilized cells) with anti-cubilin antibody (19) and anti-Tf receptor antibody R117 (25), followed by a 1-h incubation period with Alexa 488-conjugated secondary anti-mouse or anti-rabbit IgG (Molecular Probes) diluted 1:200 in the same respective buffer. The slides were washed with PBS, mounted in Dako fluorescent mounting medium, and examined with a Zeiss LSM-510 confocal microscope.

**Uptake of Tf in Rat Yolk Sac Epithelial Cells.** Virus-transformed yolk sac epithelial cells (24) were grown to confluence in 12- or 24-well plates (Nunc and Life Technologies, Grand Island, NY) in minimum essential medium (Life Technologies) containing 10% FCS. After washing, the cells were preincubated for 30 min in serum-free MEM supplemented with 0.5% ovalbumin before incubation with labeled Tf. Tf was labeled in nitriloacetate with $^{59}Fe^{3+}$ ($\approx 2$ $\mu$Ci/mg Tf) or saturated with $Fe^{3+}$ and iodinated with $^{125}I$ (20 $\mu$Ci/$\mu$g Tf) by the chloramine-T method as described (26). Cell-associated radioactivity was estimated by the lysis and counting of the radioactivity of the washed cell layer. Degradation of labeled protein was measured by precipitation of the incubation medium with 12.5% trichloroacetic acid.

## Results

**Identification of Tf as a Cubilin Ligand.** We have previously reported that cubilin-affinity chromatography of human serum leads to elution of several proteins (Fig. 1*A*) (13). The proteins of 28 kDa (apolipoprotein A1), 80 kDa, and 90 kDa represent specifically eluted proteins, whereas the proteins of 30 kDa and 67 kDa (probably albumin) also, to some extent, are seen in the eluate from a blank Sepharose column. Amino-terminal sequencing of the abundant 80-kDa protein (arrow in Fig. 1*A*) now revealed the sequence Val-Pro-Asp-Lys-Thr-Val-Arg-Trp-*X*-Ala, which is identical to the amino-terminal sequence of the 80-kDa human Tf molecule. In accordance with cubilin being a specific renal binding site for Tf, cubilin was eluted by Tf-affinity chromatography of solubilized renal brush-border membranes (Fig. 1*B*). Binding of purified Tf to cubilin as measured by surface plasmon resonance analysis (Fig. 1*C*) estimated a $K_d$ of 20 nM when assuming one class of binding sites. No measurable difference in binding affinity of Fe-saturated Tf compared with partially Fe-saturated Tf was observed (not shown). No specific binding was seen when $Ca^{2+}$ in the binding buffer was complexed to EDTA (not shown).

**Renal Uptake of Tf.** Cubilin and megalin are strongly expressed at the apical site of the proximal tubule cells in the kidney, which is a major organ of Tf clearance (10). To evaluate the role of
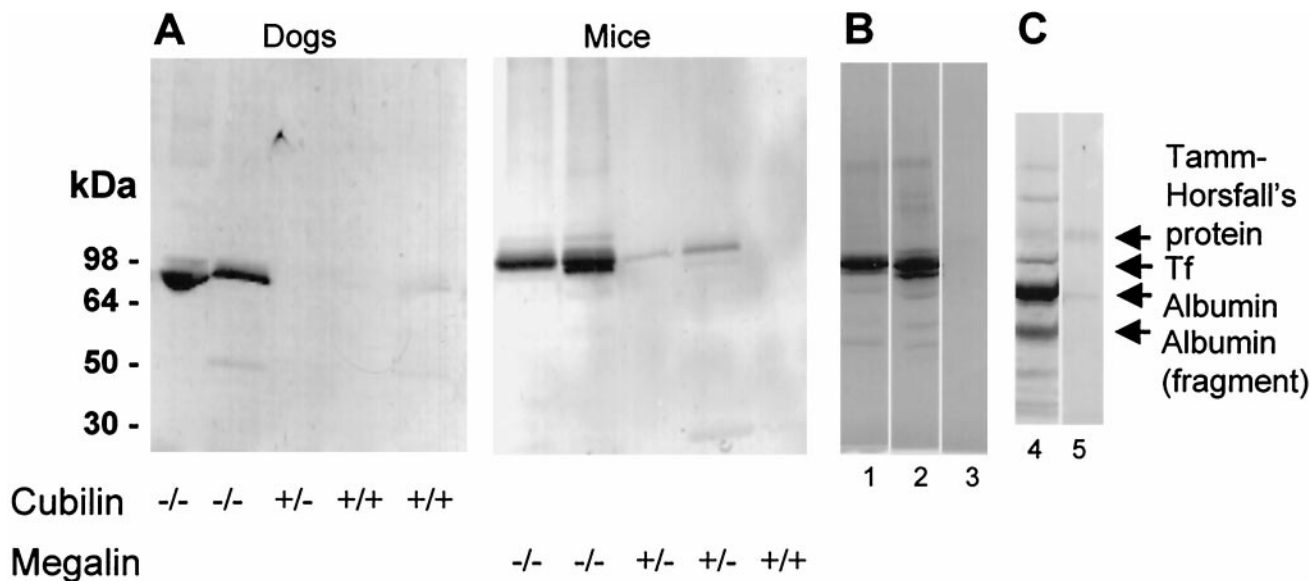
**Fig. 4.** Detection of Tf in urine of dogs with deficient surface expression of cubilin, in mice with deficient megalin expression, and in patients with Imerslund–Gräsbeck's syndrome. (*A*) Western blotting (nonreducing conditions) of 20-$\mu$l urine samples shows a high urinary content of Tf in animals homozygous ($-/-$) for cubilin or megalin deficiency, but not in heterozygous animals or control animals. (*B*) Western blotting for Tf in urine (2 $\mu$l) of two French children with Imerslund–Gräsbeck's disease (lanes 1 and 2) and in a control individual (lane 3). (*C*) Coomassie staining of 2 $\mu$l of urine from one of the Imerslund–Gräsbeck's disease patients with proteinuria (lane 4) and a control (lane 5). The filtered proteins and cubilin ligands, albumin and transferrin, are abundant proteins in the patient urine but not in normal urine. Also, several low molecular weight proteins are seen in the patient urine. The distale tubule protein, Tamm Horsfall's protein, is present in similar concentrations in patient and control urine.

cubilin and megalin in this process, we investigated the kidneys of dogs (21) deficient in functional expression of cubilin (Fig. 2) and the kidneys of megalin knockout mice (22) (Fig. 3). The dogs, which model the human Imerslund–Gräsbeck's disease, have a defect in processing cubilin (21), leading to an abnormal accumulation of cubilin in intracellular vesicles (Fig. 2*B*) instead of the tubular surface expression seen in normal dogs (Fig. 2*A*).

Immunohistochemistry of normal canine (Fig. 2*C*), human (Fig. 2*E*), and mouse kidney (Fig. 3*C*) showed, in accordance with a substantial Tf uptake, a distinct intracellular labeling of Tf concentrated in vesicular structures of the epithelial cells. Electron microscopic immunogold labeling detected apical endosome-like vesicles and electron-dense lysosomes (Figs. 2*F* and 3*C*, *Inset*).

No vesicular staining of Tf was detected in proximal tubules of the dogs and mice with failure in expression of cubilin (Fig. 2*D*) or megalin (Fig. 3*D*), respectively. However, the megalin-deficient mice (Fig. 3*D*), but not the cubilin-deficient dogs (Fig. 2*D*), exhibited staining for Tf in the apical plasma membrane below the brush-border zone. This part of the apical membrane represents normally the cubilin- and megalin-expressing coated invaginations in the crypts of the protruding microvilli (27). The *Inset* of Fig. 3*D* is an electron microscopic immunogold labeling showing the gold particles in a coated intermicrovillar invagination of the membrane. This location of Tf is consistent with binding of Tf to cubilin, which remains expressed in the intermicrovillar membrane after disruption of the megalin gene (Fig. 3*B*).

Western blot analysis (Fig. 4*A*) of urine from the cubilin-deficient dogs and megalin-deficient mice revealed that the lack of vesicular accumulation of Tf was associated with a high excretion of Tf. Virtually no excretion of Tf was seen in normal control animals. Highly increased renal excretion was also seen in human Imerslund–Gräsbeck's disease patients with strong proteinuria (Fig. 4*B*). Protein staining of the urine (Fig. 4*C*) showed that Tf, next after albumin, is one the most predominant proteins. This finding, together with the high lysosomal accu-

mulation of Tf in the normal proximal tubules, indicates that a substantial amount of Tf undergoes renal filtration and reabsorption. Western blotting revealed no differences in plasma Tf concentration in cubilin-deficient dogs versus normal dogs or in megalin-deficient mice versus normal mice (data not shown).

**Uptake of Alexa 594-Tf, ^{125}I-Tf, and ^{59}Fe-Tf in Yolk Sac Cells.** Immortalized yolk sac epithelial cells expressing high levels of cubilin and megalin (24) were used to further analyze cubilin/megalin-mediated Tf endocytosis.

Confocal microscopy of yolk sac cells preincubated with fluorescent Tf (Alexa 594-Tf) at 4°C showed a uniformly distributed punctate surface staining, which colocalized with the staining for cubilin and megalin (not shown). Fig. 5*A* shows the staining of Tf and cubilin after heating to 37°C for 1, 5, and 10 min. This experiment indicates that Tf labeling initially colocalizes with cubilin but subsequently accumulates in cubilin-negative vesicular compartments, possibly late endosomes or lysosomes. Similar staining as that at the 10-min point was seen after 15 and 30 min (not shown). TfR was also expressed in the yolk sac cells (Fig. 5*B*) but with a pronounced cell-to-cell variation, which may be because of the well-known cell cycle-dependent expression of TfR (28, 29). A similar variation of cubilin and megalin expression was not noticed. Interestingly, cells with high TfR expression had no detectable accumulation of Tf (Fig. 5*B*), maybe because of a high capacity for recycling of apoTf in these cells.

Using ^{125}I-labeled Tf, we observed that the high uptake of Tf was followed by the appearance of ^{125}I-labeled degradation products in the medium after about 30 min (Fig. 6*A*). The degradation of ^{125}I-Tf in the yolk sac cells was strongly decreased in the presence of the lysosomal proteolysis inhibitors leupeptin and chloroquine (Fig. 6*B*). Instead, cellular radioactivity accumulated in the cells. Uptake and degradation of ^{125}I-Tf were saturable and inhibited by anti-cubilin and anti-megalin polyclonal antibodies (Fig. 6*C*). Apolipoprotein A1 and RAP, but not IF-B$_{12}$, inhibited uptake and degradation. Fig. 7 shows the
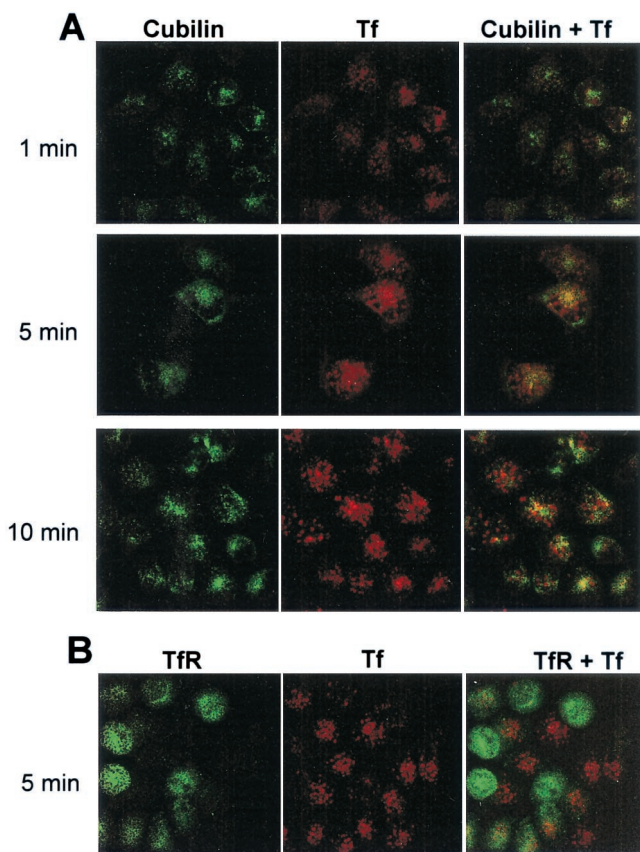
**Fig. 5.** Uptake of fluorescent Alexa 594-Tf by cultured rat yolk sac cells. (*A*) Uptake at 37°C of prebound Alexa 594-Tf (red) for 1, 5, or 10 min and immunostaining for cubilin using an Alexa 488-conjugated antibody (green). Note the initial colocalization of Tf and cubilin (1–5 min) and the subsequent vesicular accumulation of Tf in cubilin-negative structures (10 min). (*B*) Uptake at 37°C of prebound Alexa 594-Tf (red) for 5 min and immunostaining for TfR using an Alexa 488-conjugated antibody (green). Note the vesicular accumulation of Tf in TfR-negative cells.

uptake of $^{59}$Fe-labeled Tf in the yolk sac epithelial cells (Fig. 7). In this assay, which also measures the TfR-mediated internalization of Tf, the total uptake of $^{59}$Fe-Tf was reduced by ≈45% by anti-cubilin antibodies and RAP.

## Discussion

The results presented here demonstrate that cubilin, a multi-ligand receptor structurally and functionally distinct from the presently known Tf receptors, functions as a catabolic megalin-dependent Tf receptor at the apical pole of polarized epithelia cells. In the kidney, the cubilin-mediated uptake of Tf is suggested to be a biological process for rescuing iron and for supplying the iron-dependent enzymes in the renal proximal tubules (30).

The pivotal role of cubilin and megalin for Tf uptake in the kidney, which, second to the liver, is the major site of Tf catabolism (10, 30), was evidenced by studying renal handling of Tf in dogs with a cubilin-processing defect and in megalin-deficient mice. Both animal models exhibit a complete lack of Tf reabsorption, leading to a high excretion of Tf in the urine. However, in contrast to the cubilin-deficient dogs, Tf is detectable on the cubilin-expressing apical surfaces of the proximal tubules of the megalin-deficient mice. This indicates that megalin is important for cubilin–ligand internalization.

The cubilin-mediated uptake of Tf in the proximal tubules requires filtration of Tf. The apparent high filtration of Tf is
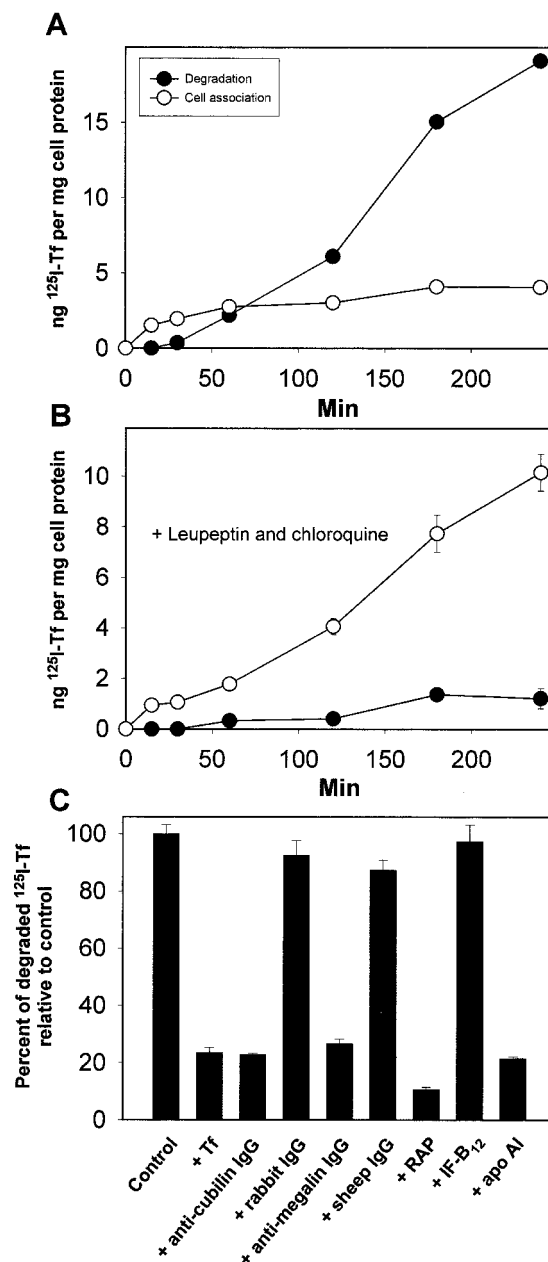


**Fig. 6.** Uptake and degradation of $^{125}$I-Tf by cultured rat yolk sac cells. Time course for cell association and degradation of $^{125}$I-Tf in the absence (*A*) or presence (*B*) of 100 $\mu$M leupeptin and 100 $\mu$M chloroquine. Degradation is measured as trichloroacetic acid-soluble $^{125}$I-labeled products released in the medium. (*C*) Degradation of $^{125}$I-Tf was assessed after 2 h at 37°C, in the presence of human Tf (1 mg/ml), human apolipoprotein (apo) A1 (1 $\mu$M), porcine IF-B$_{12}$ (1 $\mu$M), RAP (1 $\mu$M), anti-cubilin polyclonal antibody (200 $\mu$g/ml), anti-megalin polyclonal antibody (200 $\mu$g/ml), and rabbit and sheep nonimmune IgG (200 $\mu$g/ml). Data represent percent of control values (incubation with buffer alone) and are means of triplicate determinations. Standard deviations are indicated where they exceed the size of the symbols.

remarkable because the size of this protein (80 kDa) is close to the suggested size cut-off value (80–100 kDa) of proteins permeable in the glomeruli (31). However, filtration of Tf is also indicated in a recent study (32) showing Tf as an abundant protein in urine of patients with deficient renal, tubular protein reabsorption.

In contrast to the TfR-mediated uptake of Tf, where apoTf is recycled back to the surface, cubilin-mediated uptake leads to
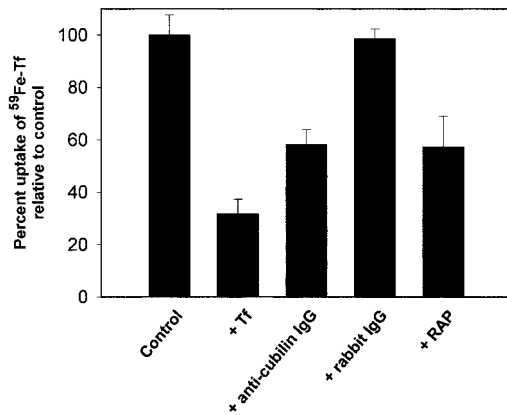
CELL BIOLOGY

**Fig. 7.** Uptake of $^{59}$Fe in immortalized rat yolk sac cells incubated with $^{59}$Fe-Tf (1500 cpm/well). Inhibition of uptake by human Tf (1 mg/ml), anti-cubilin polyclonal antibody (200 $\mu$g/ml), rabbit IgG (200 $\mu$g/ml), and RAP (1 $\mu$M). The values are the mean $\pm$ 1 standard deviation of triplicate measurements.

trapping of iron because of a higher capacity for cubilin-mediated Tf uptake than iron export by the transporters (36). We also considered the possibility that Tf might be transcytosed in the renal proximal tubules by a combined action of cubilin and TfR (apical endocytosis of Tf by cubilin, binding of apoTf to TfR in the endosomes, and recycling to the basolateral membrane). However, absent TfR expression in rat proximal tubules as investigated by immunocytochemistry (data not shown) did not support this hypothesis.

In addition to the kidney, cubilin probably also mediates uptake in the yolk sac epithelium, which is known to catabolize Tf in rodents (7). Accordingly, we measured a high cubilin-mediated Tf uptake in yolk sac-derived epithelial cells. Little is known about Tf catabolism in other epithelial tissues (37) than kidney and yolk sac. There are no known indications that cubilin should have a significant direct role for iron uptake in the intestine, where the main uptake of iron occurs by means of the duodenal DMT1 iron transporter (38). Instead, cubilin may have an indirect down-regulating effect on intestinal uptake of iron because the cubilin-mediated rescue of Tf in the kidney may contribute to maintain the level of plasma iron, which is a regulatory factor for the intestinal DMT1 expression (39, 40).

transfer of the ligand to the lysosomes. A high lysosomal uptake of iron in the proximal tubules is concordant with the renal expression of the lysosomal DMT1/NRAMP2 iron transporter (33, 34) and the MTP1 basolateral iron transporter (35). The interstitial fibrosis associated with increased glomerular permeability and iron accumulation (36) might be due to intracellular

1. de Silva, D. M., Askwith, C. C. & Kaplan, J. (1996) *Physiol. Rev.* **76,** 31–47.
2. Fleming, R. E., Migas, M. C., Holden, C. C., Waheed, A., Britton, R. S., Tomatsu, S., Bacon, B. R. & Sly, W. S. (2000) *Proc. Natl. Acad. Sci. USA* **97,** 2214–2219. (First Published February 18, 2000; 10.1073/pnas.040548097)
3. Kawabata, H., Yang, R., Hirama, T., Vuong, P. T., Kawano, S., Gombart, A. F. & Koeffler, H. P. (1999) *J. Biol. Chem.* **274,** 20826–20832.
4. Kristiansen, M., Graversen, J. H., Jacobsen, C., Sonne, O., Hoffman, H. J., Law, S. K. & Moestrup, S. K. (2001) *Nature (London)* **409,** 198–201.
5. Tolosano, E., Hirsch, E., Patrucco, E., Camaschella, C., Navone, R., Silengo, L. & Altruda, F. (1999) *Blood* **94,** 3906–3914.
6. Dautry-Varsat, A., Ciechanover, A. & Lodish, H. F. (1983) *Proc. Natl. Acad. Sci. USA* **80,** 2258–2262.
7. Young, D., Klemm, A. R., Beckman, D. A., Brent, R. L. & Lloyd, J. B. (1997) *Placenta* **18,** 553–562.
8. Odorizzi, G. & Trowbridge, I. S. (1997) *J. Cell Biol.* **137,** 1255–1264.
9. Anderson, G. J., Powell, L. W. & Halliday, J. W. (1990) *Gastroenterology* **98,** 576–585.
10. Strahan, M. E., Crowe, A. & Morgan, E. H. (1992) *Am. J. Physiol.* **263,** R924–R929.
11. Moestrup, S. K., Kozyraki, R., Kristiansen, M., Kaysen, J. H., Rasmussen, H. H., Brault, D., Pontillon, F., Goda, F. O., Christensen, E. I., Hammond, T. G., *et al.* (1998) *J. Biol. Chem.* **273,** 5235–5242.
12. Kozyraki, R., Kristiansen, M., Silahtaroglu, A., Hansen, C., Jacobsen, C., Tommerup, N., Verroust, P. J. & Moestrup, S. K. (1998) *Blood* **91,** 3593–3600.
13. Kozyraki, R., Fyfe, J., Kristiansen, M., Gerdes, C., Jacobsen, C., Cui, S., Christensen, E. I., Aminoff, M., de la Chapelle, A., Krahe, R., *et al.* (1999) *Nat. Med.* **5,** 656–661.
14. Hammad, S. M., Stefansson, S., Twal, W. O., Drake, C. J., Fleming, P., Remaley, A., Brewer, H. B., Jr. & Argraves, W. S. (1999) *Proc. Natl. Acad. Sci. USA* **96,** 10158–10163.
15. Birn, H., Fyfe, J. C., Jacobsen, C., Mounier, F., Verroust, P. J., Orskov, H., Willnow, T. E., Moestrup, S. K. & Christensen, E. I. (2000) *J. Clin. Invest.* **105,** 1353–1361.
16. Saito, A., Pietromonaco, S., Loo, A. K. & Farquhar, M. G. (1994) *Proc. Natl. Acad. Sci. USA* **91,** 9725–9729.
17. Burmeister, R., Boe, I. M., Nykjaer, A., Jacobsen, C., Moestrup, S. K., Verroust, P., Christensen, E. I., Lund, J. & Willnow, T. E. (2001) *J. Biol. Chem.* **276,** 13295–13301.
18. Sahali, D., Mulliez, N., Chatelet, F., Dupuis, R., Ronco, P. & Verroust, P. (1988) *J. Exp. Med.* **167,** 213–218.
19. Sahali, D., Mulliez, N., Chatelet, F., Laurent-Winter, C., Citadelle, D., Roux, C., Ronco, P. & Verroust, P. (1992) *Am. J. Pathol.* **140,** 33–44.
20. Biber, J., Stieger, B., Haase, W. & Murer, H. (1981) *Biochim. Biophys. Acta* **647,** 169–176.
21. Fyfe, J. C., Ramanujam, K. S., Ramaswamy, K., Patterson, D. F. & Seetharam, B. (1991) *J. Biol. Chem.* **266,** 4489–4494.
22. Willnow, T. E., Hilpert, J., Armstrong, S. A., Rohlmann, A., Hammer, R. E., Burns, D. K. & Herz, J. (1996) *Proc. Natl. Acad. Sci. USA* **93,** 8460–8464.
23. Nykjaer, A., Dragun, D., Walther, D., Vorum, H., Jacobsen, C., Herz, J., Melsen, F., Christensen, E. I. & Willnow, T. E. (1999) *Cell* **96,** 507–515.
24. Le Panse, S., Verroust, P. & Christensen, E. I. (1997) *Exp. Nephrol.* **5,** 375–383.
25. Lesley, J., Hyman, R., Schulte, R. & Trotter, J. (1984) *Cell Immunol.* **83,** 14–25.
26. Gliemann, J. & Davidsen, O. (1986) *Biochim. Biophys. Acta* **885,** 49–57.
27. Christensen, E. I., Nielsen, S., Moestrup, S. K., Borre, C., Maunsbach, A. B., de Heer, E., Ronco, P., Hammond, T. G. & Verroust, P. (1995) *Eur. J. Cell Biol.* **66,** 349–364.
28. Danova, M., Riccardi, A., Giordano, M., Girino, M., Mazzini, G., Dezza, L. & Ascari, E. (1988) *Biol. Cell* **64,** 23–28.
29. Pauza, C. D., Bleil, J. D. & Lennox, E. S. (1984) *Exp. Cell Res.* **154,** 510–520.
30. Ponka, P. (1999) *Kidney Int.* Suppl., **69,** S2–S11.
31. Brenner, B. M., Baylis, C. & Deen, W. M. (1976) *Physiol. Rev.* **56,** 502–534.
32. Norden, A. G. W., Lapsley, M., Lee, P. J., Pusey, C. D., Scheinman, S. T., Tam, F. W. K., Thakker, R. V., Unwin, R. T. & Wrong, O. (2001) *Kidney Int.* **60,** 31–37.
33. Gunshin, H., Mackenzie, B., Berger, U. V., Gunshin, Y., Romero, M. F., Boron, W. F., Nussberger, S., Gollan, J. L. & Hediger, M. A. (1997) *Nature (London)* **388,** 482–488.
34. Young, S. P. (2000) *FEBS Lett.* **466,** 135–138.
35. Abboud, S. & Haile, D. J. (2000) *J. Biol. Chem.* **275,** 19906–19912.
36. Nankivell, B. J., Tay, Y. C., Boadle, R. A. & Harris, D. C. (1994) *Kidney Int.* **45,** 1006–1013.
37. Moestrup, S. K. & Verroust, P. J. (2001) *Annu. Rev. Nutr.* **21,** 407–428.
38. Fleming, M. D., Trenor, C. C., III, Su, M. A., Foernzler, D., Beier, D. R., Dietrich, W. F. & Andrews, N. C. (1997) *Nat. Genet.* **16,** 383–386.
39. Roy, C. N. & Enns, C. A. (2000) *Blood* **96,** 4020–4027.
40. Zhou, X. Y., Tomatsu, S., Fleming, R. E., Parkkila, S., Waheed, A., Jiang, J., Fei, Y., Brunt, E. M., Ruddy, D. A., Prass, C. E., *et al.* (1998) *Proc. Natl. Acad. Sci. USA* **95,** 2492–2497.